Paper ID: FRC 100.002 | Version: v2.6

Coherence in Chaos: Diffusion, Localization, and Decoherence in the Standard Map / Quantum Kicked Rotor Family

Author: Hadi Servat

Affiliation: Independent Researcher

Contact: publish@fractalresonance.com

Website: fractalresonance.com

Abstract

> *FRC 100.002 v2.6 preserves the Standard Map / Quantum Kicked Rotor chaos program, the KAM-structure functional, localization/decoherence pilots, the Ruelle-Pollicott negative result, and the demoted stadium appendix. It records the completed registered dense classical Gate 4 test as a negative result: fine KAM-area tracking fails, while the earlier coarse zero-parameter magnitude correspondence survives in its scoped form. This route does not promote the paper as a pillar. The canonical reciprocity law remains*

> *dS + k* d ln C = 0. In this paper's declared information-nat realization k*_{mu_nat}=1, and J_sys=d[S_sys,mu+k*_{mu_nat} ln C_mu]/dt remains a system-only diagnostic, not automatically entropy production or a boundary residual.*

1. Position in the basin series and lineage

The 100 series is the basin of the FRC corpus: each paper carries the current settled statement of one foundational claim, and is updated in place as the framework moves. This document is the updated statement of 100.002. It replaces the v1 stadium-billiard paper as the carrier of the chaos claim and retains the stadium result as a demoted case study in Appendix A with its corrected caveats. Computational results — the pilot reported in §10 and the full simulation program of §12 — live in the answer appendix line FRC 100.002.001, so that the basin statement here remains stable while evidence accumulates.

Four corrections govern this version, stated up front:

1. **D ≈ 1.90 is not a pillar.** The v1 fractal-dimension value is representative, not universal, and nothing below depends on it. The KAM island hierarchy supplies textbook-real fractal motivation without a fitted exponent, but the completed dense test does not establish it as the direct carrier of Σ (§§5.4–5.5).
2. **The ledger is operationally indexed and boundary-explicit.** The canonical relation is $dS + k^* d\ln C = 0$. At the information-nat register used here, $k^*_{\mu_{\text{nat}}} = 1$ is fixed before analysis. This paper measures movement of the system-only Q diagnostic. It does not model an environment, infer entropy production, or reject the boundary-relative convention $\lambda = -d_e S$ by fiat.
3. **The load-bearing arena is the Standard Map / Quantum Kicked Rotor family**, the most standardized system in classical and quantum chaos: one drive parameter, an exact quantum counterpart, dynamical localization, a mature atom-optics experimental record including controlled decoherence, and observables hostile readers already trust.
4. **The registered classical Gate 4 route has been executed and fails.** In the frozen dense window, Σ does not track fine KAM-area variation better than entropy or the frozen area baseline. The broad magnitude correspondence survives, but this paper is not promoted as a pillar by this route, and no friendlier window will be substituted after the fact.

2. The claim

> ***Chaos is not the absence of coherence; it is an arena in which coherence structure is measurable, and in which the entropy–coherence reciprocity of the 566 line organizes what standard treatments describe piecewise.*** *Concretely: (i) in the classical mixed regime, residual coherence structure persists inside chaos and is quantified parameter-free against the exact maximum-entropy curve of 566.030; (ii) in the quantum regime, coherence built by the chaotic dynamics itself arrests the diffusion that same dynamics drives — dynamical localization read as an emergent coherence structure satisfying the operational flight criteria of 787.787 in momentum space; (iii) under decoherence, the target claim is that diffusion reopening is organized primarily by coherence-channel degradation, with strict mechanism-independent collapse still under test.*

Scope of this version. This is a corrected preprint and pilot-supported statement of the 100.002 claim. The classical dense Gate 4 test is complete and negative; its controls pass, so the fine-tracking claim is closed rather than deferred. Independent quantum routes remain open: the $t^*\gamma_C$ order-one crossover needs parameter sweeps with a defined tolerance, and the cross-mechanism collapse must be checked out of sample against the experimental record. The gates (§8), controls (§9), and kill conditions (§11) define what would promote, revise, or remove the remaining claims.

3. Operational system-only diagnostic

FRC writes the canonical relation

$$dS + k^* d\ln C = 0.$$

At a declared register μ, this may be instantiated operationally as $dS_\mu + k^*_\mu d\ln C_\mu = 0$, while its universal physical status remains conjectural. For a modeled subsystem one may write $dS_{\text{sys},\mu} = d_i S_\mu + d_e S_\mu$ and define $d_i S_\mu + k^*_\mu d\ln C_\mu = \lambda_\mu$. The identification $\lambda_\mu = -d_e S_\mu$ is admissible when it follows from that boundary convention.

This chaos paper does not model the environment. It therefore reports only

$$J_{\text{sys},\mu}(t) = \frac{d}{dt}\left[S_{\text{sys},\mu} + k^*_\mu \ln C_\mu\right],$$

with S a coarse-grained entropy and C an operational coherence measure, both fixed before any outcome is examined (§6, §9). Three points of discipline:

- $J_{\rm sys}$ diagnoses movement of the selected system-only ledger; it is not automatically d_iS, d_eS, or λ_μ.
- Where finite lag is tested, 787.787 distinguishes $\Lambda_{\rm obs}$, $\Lambda_{\rm eq}$, and optional $\Lambda_{\rm dyn}$.
- Here $\mu = \mu_{\rm nat}$ is the information-nat register and $k^*_{\mu_{\rm nat}} = 1$, declared before results. Another register requires its own predeclared unit map, not a value inferred from this dataset.

4. Symbol hygiene

Four symbols in this territory are shaped alike and must never be conflated:

Symbol	Meaning	Never confuse with
$K_{\rm drive}$	classical/experimental kick strength; tunes the map	k_*
$k^*_{\mu_{\rm nat}}$	operational representation of the starred Boltzmann bridge (1 nat here)	$K_{\rm drive}$, an outcome-fitted parameter
$J_{\rm sys}$	measured derivative of the system-only ledger	standard production or a boundary residual without a bath model
λ_μ	boundary-relative exchange/residual; may equal $-d_eS$ under a declared convention	$J_{\rm sys}$ by default
$\Lambda_{\rm obs}, \Lambda_{\rm eq}, \Lambda_{\rm dyn}$	observed transform, target, and optional latent state	the residual λ_μ

Additional working symbols: $\hbar_{\rm eff}$ (effective Planck scale of the quantum rotor), $C \in (0, 1]$ (operational coherence), S (coarse-grained entropy, nats), t^* (localization break time), γ_C (coherence decay rate), Σ (classical structure functional, §5.2).

5. Classical arena: the Standard Map and the structure functional

5.1 The map

$$p_{n+1} = p_n + K_{\rm drive} \sin x_n, \qquad x_{n+1} = x_n + p_{n+1} \pmod{2\pi}.$$

As $K_{\rm drive}$ increases: regular motion, mixed phase space with KAM islands, resonance overlap near $K_c \approx 0.9716$, global chaos, momentum diffusion. The FRC reading replaces none of this; it adds an accounting layer with an exact, pre-existing null.

5.2 The structure functional (parameter-free, anchored on 566.030)

The rotor's position variable lives on a circle, so the corpus-standard coherence channel applies directly: $C = |\langle e^{ix} \rangle|$, the mean resultant length — the Kuramoto order parameter, the same object that is $C(\kappa) = I_1(\kappa)/I_0(\kappa)$ in 566.030. For fixed C, the maximum-entropy distribution on the circle is von Mises, with entropy $S_{\text{vM}}(C)$ known in closed form (566.030 §4). Define the **structure functional**

$$\boxed{\Sigma(t) \;=\; S_{\text{vM}}\big(C(t)\big) \;-\; S\big(x(t)\big) \;\geq\; 0.}$$

The inequality is a theorem (max-ent), not a finding — which is precisely its value: Σ is a properly signed, zero-free-parameter measure of *how much organization the phase marginal carries beyond what its coherence alone requires*. $\Sigma = 0$ means the ensemble sits on the exact Bessel curve published in 566.030 before this paper existed; $\Sigma > 0$ is coherence structure inside chaos, in nats. Equivalently $\Sigma = -\Delta Q$, the vertical distance below the exact $Q(C)$ curve, so the classical ledger of this paper is literally an overlay on the 566.030 figure.

5.3 Pre-registered readings

- **Globally chaotic regime** ($K_{\text{drive}} \gtrsim 5$): $\Sigma(t)$ is transient — a filamentation spike as the initial structure is stretched, then decay to the max-ent curve as the marginal equilibrates.
- **Mixed regime** ($K_{\text{drive}} \sim 0.5$–$2.5$): $\Sigma(\infty) > 0$ persists. The original coarse sweep decreases with drive and remains consistent with the broad loss of regular structure, but the completed dense test rejects direct fine KAM-area tracking as the Gate 4 discriminator (§5.5).

5.4 The fractal, relocated honestly

The v1 intuition — that the fractal side of FRC lives in chaos — survives only as scoped motivation, not as an established carrier. The KAM island-around-island hierarchy is a textbook-real self-similar object and carries no fitted D ≈ 1.90 exposure. But the completed island-area comparison does not support the stronger claim that fine variation in Σ directly tracks survival of that hierarchy. The coarse magnitude correspondence remains; the direct fractal-carrier inference does not. Criticality remains a deeper conjectural fusion point (fractal across scale, entanglement across space, joined at the transition), but that statement belongs to the 826 line and is only pointed to here.

5.5 Dense KAM Gate 4 — executed and failed (results-negative-kept, 2026-07-12)

The registered test froze a geometry-selected window $1.45 \le K_{\text{drive}} \le 1.55$ and then measured ten unseen confirmation conditions at spacing 0.01. **Gate 4 fails.** The rank relation between measured structure and regular area is $\rho_\Sigma = 0.030$ with one-sided permutation $p = 0.477$; the condition-resampling stability interval for the rank advantage over negative entropy is entirely negative, $[-1.765, -0.128]$. This interval describes stability across adjacent fixed K conditions, not a population confidence interval.

The broad magnitude result survives in scope: the zero-fitted-parameter geometry predictor has 8.7% median relative error. It does not win the gate because the frozen one-parameter area baseline is better at 6.6%. Grid/time convergence, estimator floor, seed precision, and the fixed-area arrangement null all pass. The failure therefore closes this registered realization: fine geometric structure does not transfer into the rank of measured Σ, and the result may not be repaired by selecting another window after seeing the confirmation. This leaves 100.002 as a scoped chaos application with a coarse geometric correspondence, not a pillar promoted by the classical KAM route. The full protocol, report, code, seed-level outputs, and review notes are published with FRC 100.002.001 v1.5 under `gate4/`.

5.6 The classical decay-rate anchor — executed, and retracted as a coherence-channel test (results-negative-kept, 2026-07-08)

This anchor was pre-registered as: the decay rate of the coherence channel $|\langle e^{ix_n} e^{-ix_0}\rangle|$ equals the leading Ruelle–Pollicott resonance of the transfer operator (Venegeroles 2008), with pilot empirical rates $\gamma \approx 0.152$/kick at $K_{\text{drive}} = 5$ and $\gamma \approx 0.418$/kick at $K_{\text{drive}} = 10$ as the targets. The test was run properly and **does not pass as stated; the pilot rates are not resonances.** Three checkable facts:

1. **The pilot rates are packet transients.** Reproduced (0.150/0.463) — but they measure the spreading of a concentrated non-equilibrium ensemble (the pilot starts $p \approx 0$ on a momentum line, x concentrated, and fits $n \in [1, 12]$), not the asymptotic correlation decay from the invariant measure.

1. **The bare phase autocorrelation is analytically resonance-blind on the torus.** The one-step correlation from the uniform invariant measure is exactly zero, $\langle e^{i(x_1 - x_0)}\rangle = \langle e^{ip_0}\rangle \langle e^{iK \sin x_0}\rangle = 0 \cdot J_0(K) = 0$ (p_0 uniform, independent of x_0); numerically it drops to the finite-N floor in one step and is noise thereafter. The e^{ix} mode cannot carry the leading resonance.

1. **The true leading resonance is a different, faster object.** Computed from first principles as the leading eigenvalue of the Fourier–Bessel Koopman matrix —

$U\,e^{i(mx+np)} = \sum_l J_l((m+n)K)\,e^{i((m+l)x+(m+n)p)}$ — the leading Pollicott–Ruelle resonance is $|z_1| \approx 0.4$, $\gamma \approx 0.8$–0.95 at $K = 5, 10$ (truncation-converged up to the residual dependence of a non-compact operator). It is $\sim 5\times$ faster than the pilot transient and corresponds to a specific eigenmode combination, not the bare e^{ix}.

Disposition. The claim "the coherence-channel (phase-autocorrelation) decay rate is the leading resonance," and the specific values $0.152/0.418$, are **retracted** — they were a finite-window artifact of a mis-specified observable, caught by executing the registered test. The transfer-operator leading resonance ($|z_1| \approx 0.4$) stands as a separate, first-principles characterization of the map. A corrected coherence-channel↔resonance identity — projecting the coherence observable onto the leading Koopman eigenmode — is registered for the answer appendix (100.002.001); it is not claimed here. This retraction touches nothing else: the Σ structure functional (§5.2), the localization results, and the 566 ledger are independent of it. (Report and scripts: `output/probe/FRC-100-002-001-RP-2026-07-08/`.)

6. Quantum arena: the Kicked Rotor, localization as coherence structure

6.1 The system

$$H = \frac{p^2}{2I} + K_{\text{drive}} \cos x \sum_n \delta(t - nT),$$

whose classical limit is the Standard Map and whose quantum evolution exhibits the decisive triplet: early classical-like diffusion, arrest by **dynamical localization** at break time t^*, and restoration of diffusion under decoherence. All three are experimentally realized in atom optics (Moore et al. 1995; Ammann et al. 1998; Klappauf et al. 1998, and the modern line through the Lille Anderson-transition experiments and interaction-driven breakdown, Cao et al. 2022).

6.2 Fixed channels and the anti-circularity control

The ledger requires two channels that are demonstrably not one function of each other. The Ising c-function gate (840.102 line) killed a prior FRC claim precisely because coherence and the flowing quantity closed on each other by definition; that failure mode is named here as a mandatory control.

- **Coherence channel C**: ensemble purity $\mathrm{Tr}\,\rho^2$ of the noise-averaged density matrix (primary; operational, continuous with the existing pilot line), with nearest-off-diagonal momentum coherence $\sum_m |\rho_{m,m+1}|$ as the secondary interference channel.

- **Entropy channel S**: Shannon entropy of the **coarse-grained diagonal** momentum distribution (bin width fixed in advance) — a population measure deliberately distinct from any functional of the full spectrum of ρ.
- **Identity check (named control)**: plot S against $-\ln C$ across all runs. If the points collapse to a single curve, the ledger is algebra, not physics, and the quantum claim is void. Passing looks like what the pilot found (§10): at zero noise, S grows from 0 to ~1.6 nats while C stays pinned at 1 — a vertical branch no function can produce.

6.3 Localization read through 787.787

FRC 787.787 defines Lambda-Flight operationally: a structure is in flight if its internal coherence stays above threshold, its radius grows slower than the diffusive $\sqrt{2dDt}$, and its residual motion is predicted by the coherence gradient. The dynamically localized rotor satisfies the first two conditions verbatim, in momentum space: coherence holds near 1 while the momentum variance arrests against the classical diffusion it initially tracked. **Dynamical localization is an emergent coherence structure — order the chaotic dynamics itself builds through interference — and it is the first canonical, exactly simulable testbed for 787.787's flight criteria.** This paper therefore tests 787's predictions, not only 566's ledger.

6.4 The coherence-lifetime criterion (operational form of 787's flight/collapse condition)

787's collapse threshold says coherent transport fails when the coherence layer can no longer keep up with the structure. For the kicked rotor the operational translation is one dimensionless number:

$$\boxed{\text{decoherence crossover governed by } t^* \gamma_C = O(1).}$$

where t^* is the zero-noise break time and γ_C the early-window decay rate of the coherence channel under noise. Interference needs $\sim t^*$ kicks to build the localized state; if coherence dies faster than that, the structure never assembles and diffusion continues. The pilot brackets an order-one crossover: material reopening is already visible near $t^*\gamma_C \approx 0.5$, while the next resolved points sit near $2\text{-}3$. A sharp onset and tolerance band require the appendix sweep; this release does not claim them.

6.5 The cross-mechanism collapse

The ledger target is that diffusion reopens because the coherence channel is degraded. The strong version says the reopening magnitude is a **single function of coherence degradation, independent of the physical mechanism doing the degrading**: kick-phase noise, kick-amplitude noise, spontaneous emission, or interactions. Plotted against γ_C, all mechanisms would fall on one curve. This is the Gate-4 "many sweeps, one curve" target, not yet a passed result; the pilot reports both preliminary collapse and a low-noise mechanism split.

7. Junction: what 100.002 supplies to the corpus

Paper	Core claim	What 100.002 supplies
566 / 566.030	canonical reciprocity plus operational bookkeeping; exact system-only Q curve	a chaos-family system-only diagnostic with an exact max-ent anchor
100.003	collapse is phase-locking into attractor basins	a concrete chaotic basin geometry (mixed phase space) where locking, basin structure, and decoherence are simulable
100.009	local reciprocity storage, explicit sources/sinks, and closure residual	the global system-only diagnostic with spatial flux integrated out
787.787	Lambda-Flight: coherence transport, relaxation law, flight/collapse criteria, six failure conditions	the first canonical testbed: localization = flight in momentum space; the $t^*\gamma_C$ criterion; the hysteresis prediction (P4) testable by noise up/down sweeps

8. Gates for pillar status

Passing all four would promote this document from candidate to established pillar. The classical KAM realization of Gate 4 has now failed; the paper is not promoted by that route:

1. **Canonical arena**: Standard Map / Quantum Kicked Rotor load-bearing; stadium demoted (Appendix A).
2. **Fixed observables before results**: S, C, J_{sys}, Σ, γ_C, t^* all defined above, before outcomes; one primary coherence channel per regime, robustness channels secondary; no post-hoc switching.
3. **Cross-regime win**: the same ledger organizes classical diffusion (via Σ), localization (via the flight reading and $t^*\gamma_C$), and decoherence (via the cross-mechanism collapse).
4. **Better-than-baseline**: the classical $\Sigma(\infty)$-versus-KAM route is **FAILED and closed** (§5.5). Independent routes remain registered: the $t^*\gamma_C = O(1)$ crossover predicts the delocalization noise strength after a tolerance band is set; the reopening-vs-γ_C collapse holds across mechanisms including published experimental data; or a classical coherence observable matches an appropriately projected transfer-operator

mode. Unless one of those survives its own frozen baseline, this paper remains an application, not a pillar.

9. Controls and nulls

1. **Identity check** (§6.2) — mandatory; failure voids the quantum ledger. *[DONE in pilot as a zero-noise quantitative sanity check plus plotted channel scan: entropy span > 1 nat while purity remains pinned; full non-collapse statistic across all runs is appendix work.]*
2. **Shuffled/randomized-kick control**: deterministic structure destroyed while kick statistics preserved; Σ and the ledger structure must vanish. *[DONE in pilot as the matched stochastic null; passes. Note: temporal shuffles are the null for correlation/RP quantities, not for the one-time functional Σ.]*
3. **Matched stochastic diffusion null**: no deterministic structure; must not reproduce $\Sigma(\infty) > 0$ or the collapse. *[DONE in pilot; passes. Variance-matched variant registered for the appendix.]*
4. **Coarse-graining sweep**: entropy bins and windows varied; sign/threshold structure must be stable. *[DONE in pilot for Σ, M = 36–144; passes. Quantum bin sweep: appendix.]*
5. **$\hbar_{\text{eff}}$ sweep**: separate quantum interference from discretization artifact. *[Appendix.]*
6. **Finite-N / finite-R floors**: the classical overlay is read only above the $3/\sqrt{N}$ coherence floor; Σ bias calibrated on synthetic von Mises draws *[DONE]*; the quantum purity floor $1/R$ and the γ_C sampling bound are stated wherever they bind *[DONE for R = 32; larger R: appendix]*.
7. **Pre-registration**: all thresholds (t^* definition, γ_C window, bin widths) fixed in the analysis scripts before sweeps are extended.

10. Evidence status — 2026-07-12

Reproducible pilot scripts, seeds, JSON metrics, and figures accompany this preprint (`pilot_classical.py`, `pilot_quantum3.py`, `nulls_classical.py`). The dense classical Gate 4 result is a completed registered appendix test; the quantum results remain pilot-level. Wins, kills, and open tensions are reported at equal volume.

Classical (Standard Map, N = 4x10^4, 300 iterations, ensembles started on the max-ent curve):

- Exact-curve cross-check passes: the implementation reproduces the published 566.030 table (Q = 0.9275 at C = 0.622 vs published 0.928).
- **Estimator calibration (control a, done):** on exact synthetic von Mises samples, the Sigma estimator bias is <= 0.0017 nats across M = 36/72/144 bins, matching the

(M-1)/2N histogram theory — an order of magnitude below the mixed-regime signals. Reported Sigma values below are bias-corrected.

- Mixed regime coarse sweep: Sigma(inf) > 0 persists and decreases with drive — ~0.034 nats at K = 0.6, 0.011 at K_c, 0.0091 at K = 1.4, 0.0086 at K = 2.0, 0.0027 at K = 2.5. The later zero-parameter geometry comparison retains an 8.7% median magnitude error in the frozen dense window, but direct fine KAM tracking fails: $\rho_\Sigma = 0.030$, $p = 0.477$, and the area baseline is better (6.6% versus 8.7%).
- **Matched stochastic diffusion null (control b, done):** with the kick's deterministic x-dependence destroyed (kick phase resampled uniformly per particle per step), the null loses all phase coherence (C(inf) ~ 0.004, below the 0.015 finite-N floor) and carries no persistent Sigma at any mixed-regime K where the true map holds C(inf) = 0.12-0.34 with Sigma(inf) > 0. Caveat recorded: this null matches the kick statistics, not the diffusion coefficient (the true map's D is island-suppressed at these K); a variance-matched variant is registered for the appendix.
- **Coarse-graining sweep (control c, done):** Sigma(inf) is stable across M = 36/72/144 (e.g., K = K_c: 0.0113 / 0.0114 / 0.0118 nats). Sign and ordering unchanged.
- Globally chaotic regime: Sigma is transient (filamentation peaks ~0.34 nats at K = 2, 0.10 at K = 5, 0.02 at K = 10, then decay to the curve within estimator noise).
- Empirical phase-correlation decay rates recorded (0.152/kick at K = 5, 0.418/kick at K = 10). **The RP match was executed (§5.6, 2026-07-08) and these rates are retracted as resonances** — they are packet-spreading transients; the bare phase autocorrelation is resonance-blind on the torus invariant measure, and the true leading transfer-operator resonance is $\gamma \approx 0.8\text{–}0.95$ (~5× faster). Results-negative-kept.

Quantum (kicked rotor, K_drive = 5, hbar_eff = 1, 512 momentum levels, R = 32 realizations, 200 kicks; uncertainties: split-half spread for gamma_C, SEM over realizations for reopening):

- Zero noise: diffusion arrest at t* ~ 51 kicks with purity pinned at 1 while coarse momentum entropy grows to ~1.6 nats — the identity check passes the stored zero-noise sanity criterion; localization meets 787's flight conditions 1-2 in momentum space.
- Coherence-lifetime criterion, with uncertainties: t* gamma_C = 0.48 +/- 0.01 -> reopening 1.88 +/- 0.06 (phase) and 0.46 +/- 0.02 -> 1.66 +/- 0.04 (amplitude); t* gamma_C = 2-3 -> reopening 4.5-4.9; t* gamma_C >> 1 -> 9-16x. The pilot brackets an order-one crossover, but onset is unresolved between roughly 0.5 and 2-3; no tolerance band is claimed until the appendix sweep.
- Cross-mechanism collapse: preliminary and tensioned — consistent with a shared increasing curve in the resolved region, but with an **open tension reported at full**

volume: at matched gamma_C ~ 0.009 the reopenings differ by ~3 sigma (1.88 +/- 0.06 phase vs 1.66 +/- 0.04 amplitude). Either the collapse has a small mechanism-dependent residual at low noise, or the gamma_C estimator (purity, early-window fit) is not yet the right abscissa there. The appendix must resolve this; the strict one-curve claim is NOT yet passed.

- Resolution limit recorded: gamma_C saturates at the channel-sampling bound (1/EVERY = 0.25/kick) for sigma >= 0.1 (phase) / 0.2 (amplitude); the high-noise end of the collapse plot is bounded, not measured. Finer sampling registered for the appendix.

Kills recorded in this revision (this paper's own instruments, falsified by its own runs):

- **Kill A**: the l1-normalized off-diagonal coherence gauge is non-monotonic under localization-length growth — a badly designed instrument, dropped. Purity retained as primary.
- **Kill B**: the naive differential prediction "white amplitude noise does not reopen diffusion" is false — at matched sigma, per-kick amplitude jitter and phase jitter reopen diffusion almost identically. The experimental amplitude-noise robustness in the atom-optics record (quantum resonances, colored-noise regimes) does not transfer to white per-kick jitter, and this paper does not claim it. What survives — and is stronger — is the mechanism-collapse claim of §6.5, now itself under tension at low noise (above) and awaiting the out-of-sample test against the published record (Ammann 1998; Klappauf 1998; Steck dissertation ch. 4; White–Ruddell–Hoogerland 2014; Cao 2022), mechanism by mechanism, with the coherence measure each experiment actually reports.

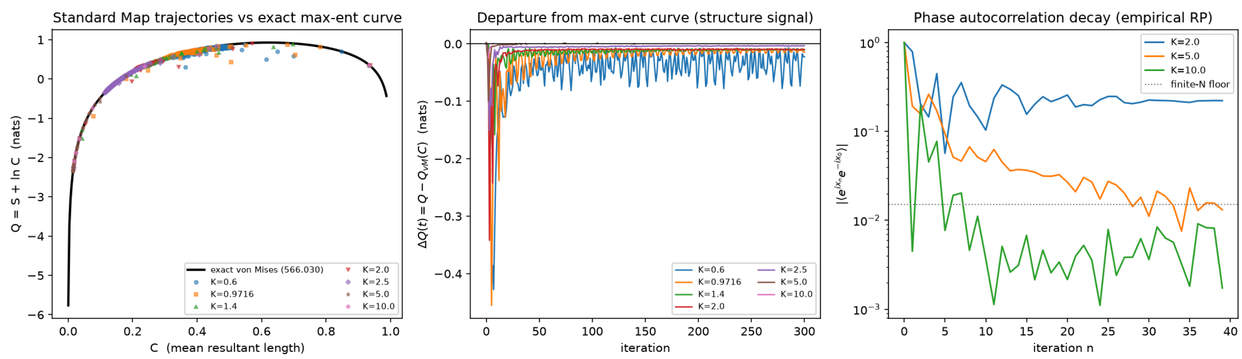

Figure 1. Classical Standard Map trajectories against the exact von Mises ledger curve, with structure-functional and empirical RP diagnostics.

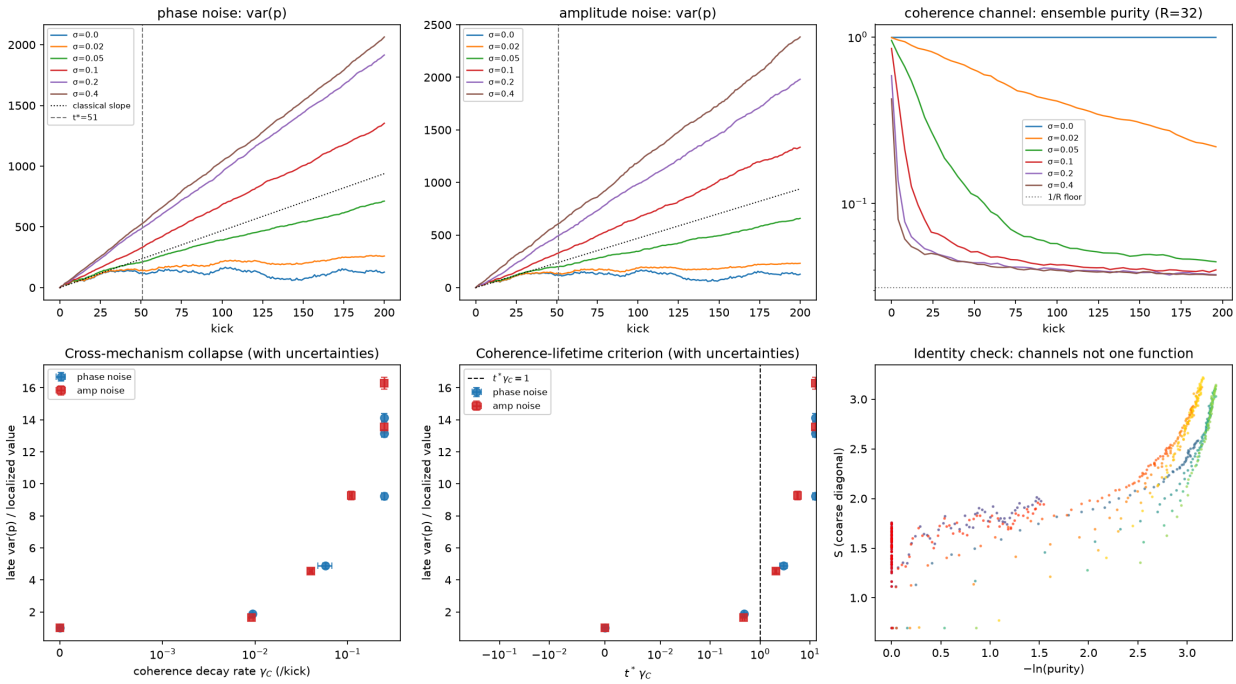

Figure 2. Quantum kicked-rotor channels: diffusion reopening, purity decay, cross-noise collapse, lifetime criterion, and identity check.

10a. Data and code availability

Pilot values are produced by the accompanying scripts with fixed seeds. Dense Gate 4 values come from the retained protocol, scripts, JSON outputs, and report in FRC 100.002.001 v1.5; no confirmation point was removed. This release package includes rendered HTML/PDF and a checksum manifest. Pilot scripts create a scratch `results/` directory when rerun. JSON metrics are compared with `pilot/compare_metrics.py`, which uses relative and absolute tolerances so near-zero floating-point values do not create false failures.

File	Role
`FRC-100-002-v2.6.md`	this paper
`FRC-100-002-v2.6.html`, `FRC-100-002-v2.6.pdf`	rendered publication files
`render_frc_html_pdf.py`, `requirements.txt`	local renderer and pinned Python dependencies
`pilot/pilot_classical.py`	Standard Map overlay, structure functional, empirical RP rates
`pilot/pilot_quantum3.py`	kicked rotor, channels, criterion, collapse,

	uncertainties (R = 32)
`pilot/compare_metrics.py`	tolerance-aware reproduction check for regenerated JSON (default rtol 1e-6, atol 1e-12)
`pilot/nulls_classical.py`	estimator calibration, matched stochastic null, coarse-grain sweep
`pilot/classical_metrics.json`, `pilot/quantum_metrics.json`, `pilot/classical_nulls.json`, `CHECKSUMS.txt`	machine-readable outputs and SHA-256 release manifest
`fig1_classical_vonmises_overlay.png`, `fig2_quantum_channels.png`	figures
`REPRODUCTION-REPORT.md`	release-regeneration commands, environment, and comparator results

11. Kill conditions

The classical fine-tracking condition has fired: $\Sigma(\infty)$ does not track fine KAM survival better than the frozen entropy and area baselines. That route is closed and cannot promote the paper. The following conditions continue to govern the independent claims:

- the identity check fails (S and $\ln C$ collapse to one function under the fixed definitions);
- the coarse $\Sigma(\infty)$ magnitude correspondence vanishes under reasonable coarse-graining or is reproduced by the shuffled/matched-noise controls;
- the delocalization crossover is not controlled by order-one $t^*\gamma_C$ after a fine sweep, or the reopening-vs-γ_C curve fails to collapse across mechanisms;
- ~~the classical coherence decay rate does not match the analytic leading Ruelle–Pollicott resonance~~ (this kill item was mis-specified — the bare phase-autocorrelation observable is analytically resonance-blind on the torus, §5.6; the corrected item is that a coherence observable *projected onto the leading Koopman eigenmode* fails to match $|z_1|$, registered for 100.002.001);
- everything above is fully explained by standard observables with no stable residual structure.

Failure of a registered route kills that route at its claimed strength. The failed classical Gate 4 route prevents pillar promotion by fine KAM tracking but does not erase the separately scoped coarse magnitude result. None of these outcomes tests or kills the 566 reciprocity line, whose own kill conditions live in the 566 papers.

12. Answer appendix program (FRC 100.002.001)

1. **Completed, FAIL:** frozen dense K_{drive} sweep of $\Sigma(\infty)$ against regular-area geometry, with seed, estimator-floor, fixed-area-null, grid, and time controls. No alternate-window search is permitted under this registration.
2. Ruelle–Pollicott match: numerical leading resonance of the transfer operator versus a coherence observable projected onto the leading Koopman eigenmode.
3. Quantum sweeps in K_{drive}, $\hbar_{\text{eff}}$, and noise; criterion tolerance band for $t^*\gamma_C$; mechanism set extended to simulated spontaneous emission and, from the literature, interactions.
4. Out-of-sample test of the cross-mechanism collapse against the published atom-optics record.
5. Hysteresis test of 787 Prediction 4: noise swept up then down at rate r; lag vs $\tau_\Lambda r$.
6. Matched stochastic and shuffled-phase nulls throughout.
7. Negative results retained in the public record as results-negative-kept.

Appendix A — The stadium billiard, demoted

The v1 stadium result is retained as a geometric case study: a multiscale perturbation of the stadium billiard altering nodal geometry, with quantum scars as the established phenomenon of residual structure in chaotic eigenfunctions. Its correct role is illustrative; its incorrect roles — central proof, universal D ≈ 1.90 signature, sole test of "chaos has structure" — are withdrawn. Any future use requires matched random-potential controls, parameter sweeps, and resolution-sensitivity analysis. The v1 record remains visible in the concept lineage with corrected caveats.

Version note

Version 2.6 records the completed negative dense Gate 4 result. Fine KAM-area tracking does not beat entropy or the frozen area baseline; the coarse zero-parameter magnitude correspondence survives, but the paper is not promoted as a pillar by this route. The Standard Map/QKR program, canonical equation, information-nat k^* stance, boundary-relative residual, and system-only status of $J_{\text{sys},\mu}$ are unchanged.

References

1. B. V. Chirikov, "A universal instability of many-dimensional oscillator systems," *Physics Reports* 52, 263–379 (1979).
2. G. Casati, B. V. Chirikov, F. M. Izrailev, J. Ford, "Stochastic behavior of a quantum pendulum under a periodic perturbation," *Lecture Notes in Physics* 93, 334–352 (1979).
3. S. Fishman, D. R. Grempel, R. E. Prange, "Chaos, Quantum Recurrences, and Anderson Localization," *PRL* 49, 509 (1982).
4. F. L. Moore, J. C. Robinson, C. Bharucha, B. Sundaram, M. G. Raizen, "Atom Optics Realization of the Quantum Delta-Kicked Rotor," *PRL* 75, 4598 (1995). DOI: 10.1103/PhysRevLett.75.4598.
5. H. Ammann, R. Gray, I. Shvarchuck, N. Christensen, "Quantum Delta-Kicked Rotor: Experimental Observation of Decoherence," *PRL* 80, 4111 (1998). DOI: 10.1103/PhysRevLett.80.4111.
6. B. G. Klappauf, W. H. Oskay, D. A. Steck, M. G. Raizen, "Observation of Noise and Dissipation Effects on Dynamical Localization," *PRL* 81, 1203 (1998). DOI: 10.1103/PhysRevLett.81.1203.
7. D. A. Steck, dissertation, ch. 4: Localization and Decoherence in the Kicked Rotor.
8. R. Venegeroles, "Leading Pollicott–Ruelle resonances for chaotic area-preserving maps," *Phys. Rev. E* 77, 027201 (2008). DOI: 10.1103/PhysRevE.77.027201.
9. D. H. White, S. K. Ruddell, M. D. Hoogerland, "Phase noise in the delta kicked rotor: from quantum to classical," *New J. Phys.* 16, 113039 (2014). DOI: 10.1088/1367-2630/16/11/113039.
10. A. Cao et al., "Interaction-driven breakdown of dynamical localization in a kicked quantum gas," *Nature Physics* 18, 1302 (2022). DOI: 10.1038/s41567-022-01724-7.
11. L. A. Bunimovich, "On the ergodic properties of nowhere dispersing billiards," *Commun. Math. Phys.* 65, 295 (1979).
12. E. J. Heller, "Bound-State Eigenfunctions of Classically Chaotic Hamiltonian Systems: Scars of Periodic Orbits," *PRL* 53, 1515 (1984).
13. H. Servat, *FRC 566.001 — Entropy–Coherence Reciprocity and UCC*. DOI: 10.5281/zenodo.17437759.
14. H. Servat, *FRC 566.030 — Reciprocity in Action: The Entropy–Coherence Current Across a Synchronization Transition*.
15. H. Servat, *FRC 100.003 — Resonant Collapse*. DOI: 10.5281/zenodo.15079820.
16. H. Servat, *FRC 100.005 — Thermodynamic Consistency*. DOI: 10.5281/zenodo.17438231.
17. H. Servat, *FRC 100.009 — Local Reciprocity Dynamics*. DOI: 10.5281/zenodo.20328893.
18. H. Servat, *FRC 787.787 — Lambda-Flight* (2026).